Novel Preparation Techniques for Thin Metal-Ceramic Composite Membranes

King Lun Yeung and Arvind Varma
Dept. of Chemical Engineering, University of Notre Dame, Notre Dame, IN 46556

Composite metal membranes obtained by supporting thin metallic films on ceramic substrates have good thermal and mechanical stability. The use of a thin metal film increases transmembrane flux, while retaining high permselectivity that is characteristic of metallic membranes. Novel techniques have been developed for preparing metal–ceramic composite membranes. By the appropriate use of osmotic pressure, the microstructure, porosity, and thickness of the deposited metal can be systematically manipulated. Three new procedures are described for film densification and fabrication: (1) the osmotic pressure is used to densify an existing supported metal membrane; (2) densification and growth of the film is managed under the influence of osmotic pressure by using a dilute plating solution; and (3) films of varying porosity are deposited on the ceramic membrane by combining electroless deposition and osmotic pressure. Silver, palladium, and palladium–silver films prepared by these techniques on a commercial alumina membrane (Membralox) are thermally more stable than similar films deposited by conventional electroless plating.

Introduction

Gases are soluble to a certain extent in metals (Barrer, 1941; Smithells, 1937) and in the presence of concentration gradient, can diffuse through it. This transport mechanism is known as *solution diffusion mechanism* (Bhave, 1991). Separation between the gases can occur due to the difference in the solubility and diffusivity of the gases in the metal. Some metals such as silver, palladium, and their alloys have been used in gas separation and purification. Such membranes usually have better permselectivity than conventional ceramic and polymeric membranes. For example, an infinite separation factor for hydrogen in a H_2/N_2 system has been reported for palladium membranes (Uemiya et al., 1988), while Collins and Way (1993) have reported a more modest value of about 650 for their palladium membrane. Similarly, silver shows high selectivity toward oxygen permeation (Wu et al., 1993). Generally, membranes made from metal foils have low permeability owing to the low diffusivity of gases through solids (cf. Holleck, 1970). In order to increase permeation while retaining the high permselectivity of dense metal membranes, it is necessary to reduce the thickness of the metallic layer. However, mechanical and thermal stability of the film usually decrease proportionally.

Recently, composite membranes made of a thin metallic layer deposited on a porous support have been reported by several workers. These membranes have high permselectivity and transmembrane flux, and exhibit good mechanical and thermal stability at high temperatures. Composite membranes made up of thin palladium films have been prepared by sputter coating onto anodic alumina substrate (Konno et al., 1988), and by electroless deposition on microporous glass (Uemiya et al., 1988), porous silver disks (Govind and Atnoor, 1991), porous stainless steel (Shu et al., 1993), and ceramic membrane (Collins and Way, 1993). Also, Gryaznov and coworkers (1993) have prepared composite membranes by depositing thin palladium alloy films on asymmetric polymer membranes, porous metal sheets, and oxide plates by sputtering.

Using electroless plating, surfaces with complex geometry can be coated with a uniform layer of metal film, for example, silver, palladium, or palladium–silver. In this article, we present three novel preparation techniques based on electroless plating. By modifying conventional electroless plating with the use of osmosis, the microstructure and porosity of the deposited metal can be systematically manipulated to give films of controlled porosity over a wide range. These tech-

---

Correspondence concerning this article should be addressed to A. Varma.

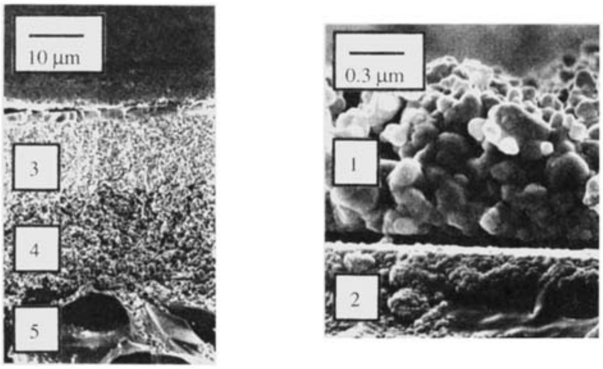

Figure 1. Cross section of a silver–Membralox composite membrane.

(1) Silver film; (2) γ-Al_2O_3 layer; (3) and (4) intermediate aluminas; (5) α-Al_2O_3 ceramic tube.

niques also improve thermal stability of the supported metal films as compared to those deposited by conventional electroless plating.

Experimental

Electroless Plating

A commercial ceramic membrane (Membralox) was used as the support for thin Ag, Pd, and Pd–Ag films. The ceramic membrane was tubular, 1 cm in diameter, and 25 cm long, with a wall thickness of about 1.5 mm. The metal film was deposited on the γ-Al_2O_3 layer located on the inside surface of the tube. Figure 1 shows a typical composite membrane made up of a thin silver film (0.8 μm) supported on the γ-Al_2O_3 layer of Membralox. The ceramic membrane itself is composed of four alumina layers of increasing porosity, ranging from the 2-μm layer of γ-Al_2O_3 membrane with a 40-Å pore size to the 1.5-mm-thick macroporous α-Al_2O_3 support. Two intermediate alumina layers, approximately 15 μm each, are sandwiched between the support and membrane layers as can be seen in the figure.

Prior to film deposition, the ceramic membrane was cut into smaller pieces about 3–4 cm long and cleaned with dilute sodium hydroxide solution to remove organic contaminants and dirt. The pieces were then rinsed repeatedly (at least three times) with deionized water and stored in a desiccator. Silver was deposited onto the membrane by electroless plating from a silver solution consisting of silver–citrate complex and formaldehyde. Palladium was deposited from palladium–ammine complex using sodium hypophosphite as the primary reducing agent. Palladium and silver were codeposited from an ammine solution stabilized by ethylenediamine tetraacetate (EDTA) using hydrazine as reducing agent. In all cases, a buffer solution was used to maintain the pH of the plating bath at 10. The compositions of the plating solutions are summarized in Table 1, and are typical of those used for electroless plating (cf. Pearlstein, 1974). The metal films were deposited on the γ-Al_2O_3 layer by circulating the plating solution through the ceramic tube using a peristatic pump (Figure 2). Tygon tubing (4.8 mm diameter) was used, giving a constant volumetric flow rate of about 120 mL/min. The plating solution was immersed in a heated water bath and its temperature was maintained within ±2°C of the setpoint.

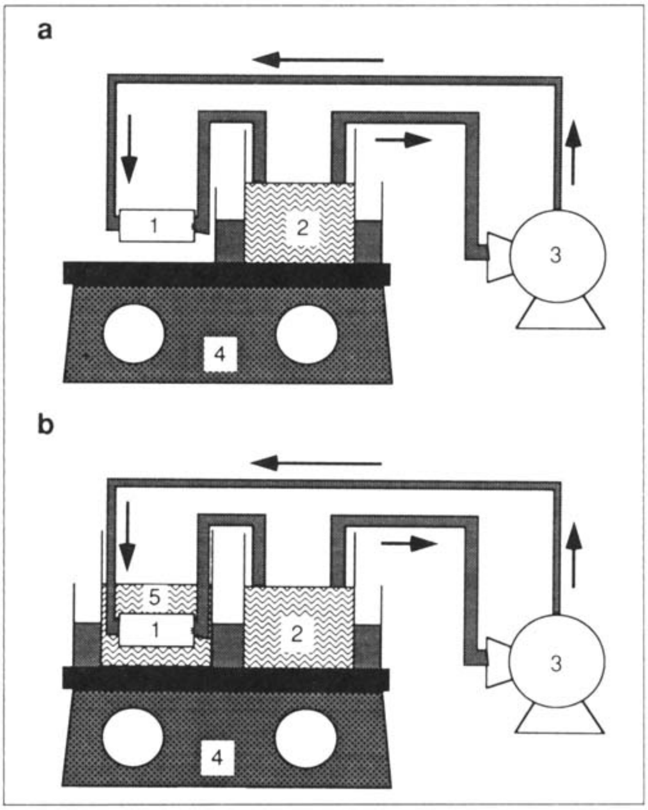

Figure 2. Experimental setup: (a) electroless plating; (b) electroless plating with osmosis.

(1) Ceramic membrane; (2) plating solution; (3) pump; (4) heater; (5) shell-side solution.

Silver was deposited at 65°C for 6 h, consuming five batches of plating solution. Owing to bath depletion, each batch (110 mL) was allowed to plate for only 75 min, with the last batch terminated after only 60 min. For palladium, only one batch

Table 1. Composition of Plating Solutions for Silver, Palladium, and Palladium–Silver Electroless Plating

Silver 1-L Plating Solution		Palladium 1-L Plating Solution		Palladium–Silver 1-L Plating Solution	
Silver nitrate	9.1 g	Palladium chloride	1.8 g	Tetraammine palladium nitrate	0.50 g
Sodium citrate	6.4 g	Ammonium hydroxide	24 mL	Silver nitrate	0.03 g
Formaldehyde (37 wt. %)	18 mL	Ammonium chloride	3.6 g	Ammonium hydroxide	200 mL
Buffer (pH 10)	91 mL	Formaldehyde (37 wt. %)	16 mL	Disodium EDTA	40.0 g
		Sodium hypophosphite	8 g	Hydrazine (1 M)	5.6 mL
		Buffer (pH 10)	80 mL	Buffer (pH 10)	100 mL

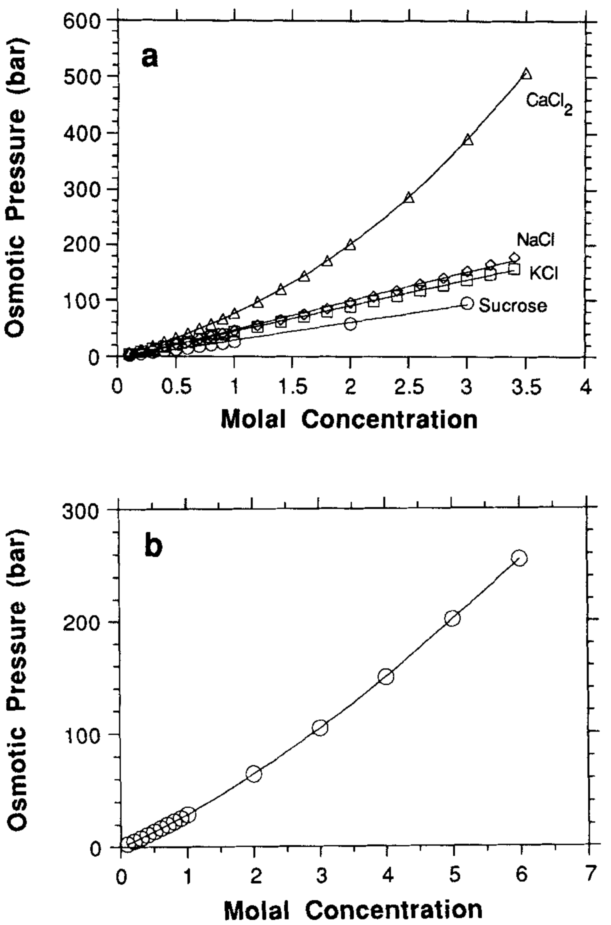

Figure 3. (a) Osmotic pressure vs. molal concentrations of various solutes in an aqueous solution at 25°C; (b) osmotic pressure vs. molal concentration of sucrose in an aqueous solution at 60°C.

of plating solution (200 mL) was used and the deposition was conducted at 55°C for 6 h. Codeposition of palladium and silver was carried out at 60°C for 6 h, consuming three batches of plating solution (200 mL/batch). More than one batch was required in this case since the effectiveness of the reducing agent, hydrazine, decreases rapidly with time.

After deposition, each membrane sample was sectioned into four pieces and rinsed with distilled water and acetone, then blow-dried with air and stored in a desiccator. Unconsumed silver and palladium remaining in the plating baths were recovered and converted to salts for reuse.

Heat treatment

The use of metallic membranes is for gas separation and reaction at elevated temperatures, hence their thermal stability is an important issue. For this, the membranes were subjected to a heat treatment study in a 12-mm-ID quartz-tube flow reactor equipped with a furnace and temperature controller. The silver-ceramic membranes were heat treated in 100 mL/min flowing oxygen at 350°C for 55 h. The codeposited palladium-silver films were heat treated in 100 mL/min flowing hydrogen at 400°C for 2 h to form a Pd/Ag alloy phase.

Structural characterization

The film microstructure was imaged using scanning electron microscopy (SEM) (JEOL JSM-T300, ISI-60A, and Hitachi FESEM S-4500). The samples were sputter coated with Pd/Au and attached to aluminum stubs using silver paint to reduce sample charging. The surface microstructure of the film was obtained both along the center and along the edge of the samples, from which the film thickness was measured.

The palladium-silver-ceramic membranes were also characterized by X-ray diffraction (XRD) using a Diano XPG 2 X-ray diffractometer with CuKα radiation source and graphite monochromator. The formation of the alloy phase from the mixed deposit of palladium and silver was determined using XRD, and its composition was calculated based on the diffraction intensities (Cullity, 1978).

Materials

The ceramic membrane was purchased from U.S. Filter, Warrendale, PA. Silver nitrate (99.9999%) and palladium chloride (99.999%) metal precursors were obtained from Aldrich Chemical Company, Inc. The complexing and reducing agents: ammonium hydroxide (28-30 wt. %), ammonium chloride, disodium ethylenediamine tetraacetate, formaldehyde (37 wt. %), hydrazine (1.0 M), hydrochloric acid (37 wt. %), sodium citrate, and sodium hypophosphite were supplied by Fisher Scientific. The sodium hydroxide (50 wt. %) and pH 10 buffer solutions were also supplied by Fisher Scientific.

Ultrahigh purity grade oxygen and hydrogen (Linde) used in the heat treatment study were further purified by passing through columns of drierite and molecular sieve to remove water moisture and hydrocarbon contaminants.

Results

Membrane preparation

We have developed a novel preparation technique for composite metal-ceramic membranes, which allows direct control over the membrane's microstructure and porosity. The technique can also be used to densify an existing membrane, reducing its porosity while enhancing thermal stability. The basic concept is the appropriate use of osmosis, either alone to modify the membrane structure, or in conjunction with a liquid phase deposition technique such as electroless plating.

The osmotic pressure can be large, depending on the concentration of the solute. For example, Figure 3a shows the osmotic pressures of different electrolytes and nonelectrolytes in an aqueous solution at room temperature (cf. Robinson and Stokes, 1959; Weast, 1986; Garner, 1930) as a function of molal concentration of the solute (that is, moles of solute per kilogram of solvent). A 3.5-m CaCl$_2$ solution has an osmotic pressure of about 517 bar, while similar concentrations of NaCl, KCl, and sucrose exert about 200, 160, and 100 bar, respectively. These magnitudes represent a relatively high pressure that is not easily obtained by other means. In addition, the osmotic pressure can be systematically varied by simply changing the amount of solute present. Sucrose so-

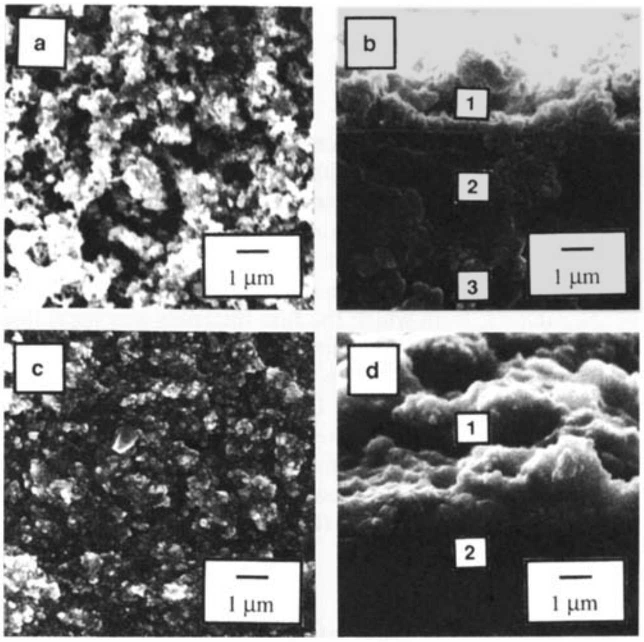

Figure 4. SEM micrographs of the film surface and cross section for (a) and (b) silver film deposited in air, and (c) and (d) after film densification in 6-m sucrose solution.

(1) Silver film; (2) γ-Al_2O_3 layer; (3) intermediate alumina.

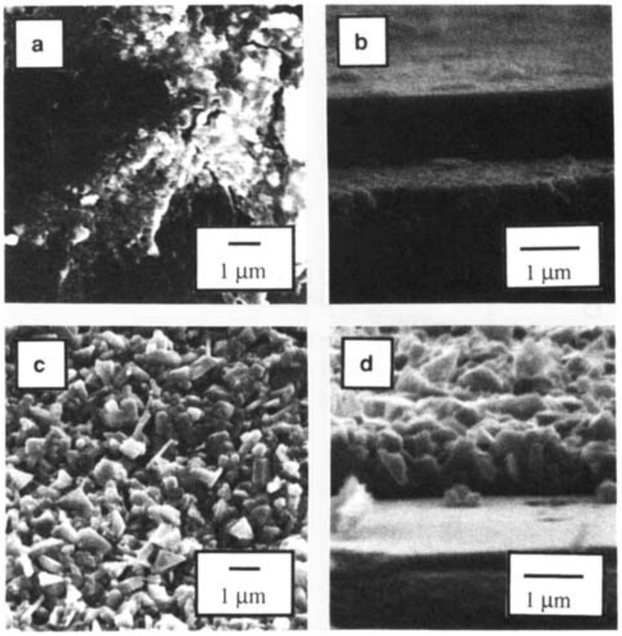

Figure 5. SEM micrographs of the film surface and cross section for (a) and (b) after subjecting the silver film deposited in air (Figures 4a and 4b) to reverse osmotic pressure (6.0-m sucrose), and (c) and (d) after subjecting the compacted film shown in Figures 4c and 4d to the same reverse osmotic pressure.

lution was used primarily in this study because of the extensive osmotic pressure data available (Garner, 1930). Figure 3b shows that at 60°C, a 3.0-m sucrose solution has an osmotic pressure of about 100 bar, while doubling the solute concentration to 6.0 m raises it to about 250 bar.

The osmotic pressure can be brought to bear on preparing supported metallic membranes by maintaining a difference in the solute concentration between the two sides of the membrane. For the case of a tubular membrane, the tube is immersed in a concentrated aqueous solution while a dilute plating solution is circulated through the tube-side. The concentration gradient between the tube-side and the shell-side solutions results in a radial osmotic pressure normal to the tube wall. A radial *outward* flux of water compresses the deposited metal against the support, while simultaneously supplying new precursor to the tube wall. Most importantly, the osmotic pressure is a colligative property that is independent of the chemistry of the solute and the membrane material, and is dependent *only* on the solute concentration in the solution (Glasstone, 1940; Atkins, 1990).

Film densification

Figure 4a shows the microstructure of a silver film deposited by a conventional electroless plating of silver on the γ-Al_2O_3 layer of the composite membrane. The film is composed of silver grains of less than 270 nm in size. Based on the SEM image, the film appears porous and has a rough surface morphology. A cross-sectional view (Figure 4b) shows that a 2.5-μm-thick silver film was deposited. The figure also shows the γ-Al_2O_3 membrane layer and the intermediate alumina layer beneath it. The film is made up of multiple layers of deposited silver grains. Immersing this membrane under 6.0-m sucrose solution while distilled water was pumped through the tube for 30 min resulted in a significant change in the film microstructure, as shown in Figure 4c. The resulting film is denser and smoother than the original film (cf. Figure 4a). Figure 4d shows that the film is 1.6 μm thick, hence thinner than the original film, and has a relatively dense structure.

If the original film is immersed instead in distilled water, while 6.0-m sucrose solution is pumped through the tube, the direction of the osmotic pressure is *reversed* from radially outward to radially inward. In this case, instead of compressing the film against the γ-Al_2O_3 support, the film is peeled off from the support by the osmotic pressure and the resulting damage can be seen in Figure 5a–5b. When the same experiment is performed on a densified film (cf. Figures 4c–d), it remains intact with no apparent damage and has thickness of about 1.5 μm (Figure 5d). Figure 5c shows that the film has quite a different microstructure than before, made up of micron-size silver crystals instead of the smaller grains found on the initial compacted film.

To determine the effect of densification time on film stability, four silver films deposited in air were densified under 6.0-m sucrose for 0.5, 1, 3 and 6 h, respectively. The film structures did not vary with densification time. To test the film adhesion and mechanical integrity, the densified films were then subjected to the same reverse experiment as earlier wherein 6.0-m sucrose was pumped through the tube for 30 min while it was immersed in distilled water. Except for

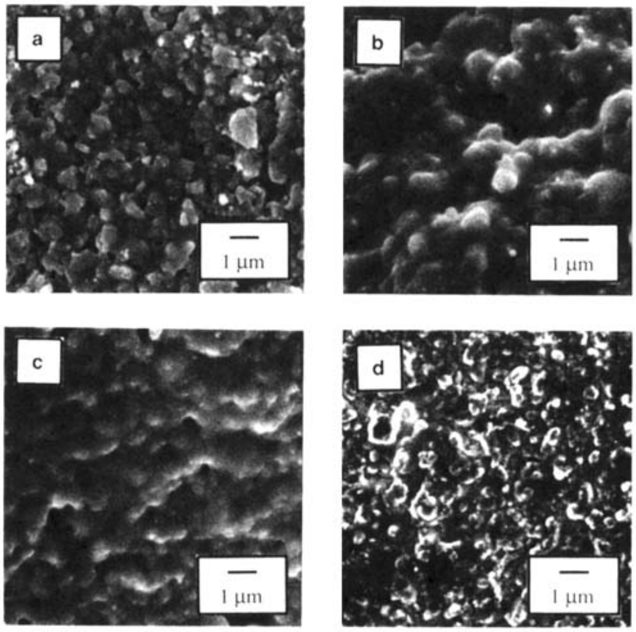

Figure 6. Film microstructures after heat treatment in oxygen at 350°C and 55 h for silver films densified for (a) 30 min, (b) 1 h, (c) 3 h, (d) 6 h.

$t = 0.5$ h (cf. Figure 5c–5d), the films did not exhibit any structural changes. These membranes were then subjected to heat treatment in oxygen at 350°C and 55 h to determine the thermal stability of the deposited films. Figure 6 clearly shows that the films densified for a longer period of time are more stable.

From the preceding experiments, it is clear that osmotic pressure is responsible for significant effects on the film microstructure, especially its porosity and grain size.

Film densification with growth

In the preceding procedure, the increase in film density was obtained at the expense of decreased film thickness. Since the stability of a film is generally proportional to its thickness, it is desirable to maintain or even increase the film thickness during the densification step. This can be achieved conveniently by starting with the film shown in Figures 4a–4b and substituting a dilute plating solution for the distilled water flowing through the tube-side while the membrane is immersed in the 6.0-m sucrose solution. Figure 7a shows that the resulting film obtained after 30 min has the same dense morphology as the compacted film shown in Figure 4c, while the film thickness measured from Figure 7b is 4.0 μm, which is about 50% thicker than the original silver film.

Simultaneous electroless plating and osmosis

Silver films. In the techniques described earlier, the deposition of silver film and its densification were carried out in two separate steps. First the film was deposited by electroless plating, and then a radial osmotic pressure was applied normal to the film, resulting in film densification. These techniques are especially useful for modifying existing membranes or for repairing damaged membranes. However, by combining the two processes, electroless plating and osmotic densification in a *single* step, one can achieve better control of the film microstructure, especially its porosity. Since the osmotic pressure depends only on the concentration gradient between the shell-side and the tube-side of the membrane, and is independent of the plating chemistry, it can be adjusted simply by changing the shell-side concentration of solute without affecting the plating processes.

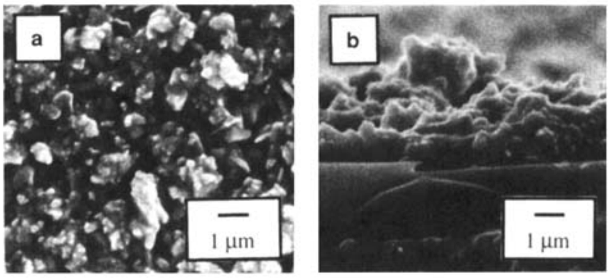

Figure 7. SEM micrographs of the (a) film surface and (b) cross section for a silver film densified with growth under 6.0-m sucrose using a dilute (1:4) plating solution.

Three silver films deposited from the *same* plating solution are shown in Figure 8. In this experiment, three ceramic membranes were linked together in series using Tygon tubing and were immersed, respectively, in a 6.0-m sucrose solution, an aqueous solution (100 mL) containing 2 mL of 37 wt. % formaldehyde, and distilled water. The plating solution was then circulated through the tubes. Figure 8a shows that under a radially outward osmotic pressure (6.0-m sucrose), the film is dense and nonporous with a smooth surface morphology. The measured film thickness (Figure 8b) is about 1.3 μm. Using the same concentration of formaldehyde in the shell-side as in the plating solution, a zero osmotic pressure was approximated. As shown in Figures 8c–8d, the film is porous and thin (0.6 μm) in the absence of radial pressure. The direction of the osmotic pressure was reversed when the tube was immersed in distilled water, and the resulting deposit is uneven and discontinuous (Figure 8e). Instead of forming a continuous film, the deposits grow radially inward leading to uneven, columnlike growths (Figure 8f). This experiment shows that while keeping the plating chemistry unchanged, one can substantially alter the film microstructure using osmotic pressure by simply changing the shell-side concentration of the solute.

Palladium films. Since the preceding technique is independent of plating chemistry, it has broad applications in membrane preparation. Supported Pd films were also prepared following the same procedure. Two Pd films were deposited in series from the *same* plating solution (see Table 1), one with the tube exposed to air (Figure 9a) and the other under 6.0-m sucrose solution (Figure 9b). Palladium deposited in air does not yield a film, but rather forms loose aggregates of palladium crystallites (about 200 nm) on the surface of the γ-Al$_2$O$_3$ support. On the other hand, under the influence of osmotic pressure, the same solution deposits

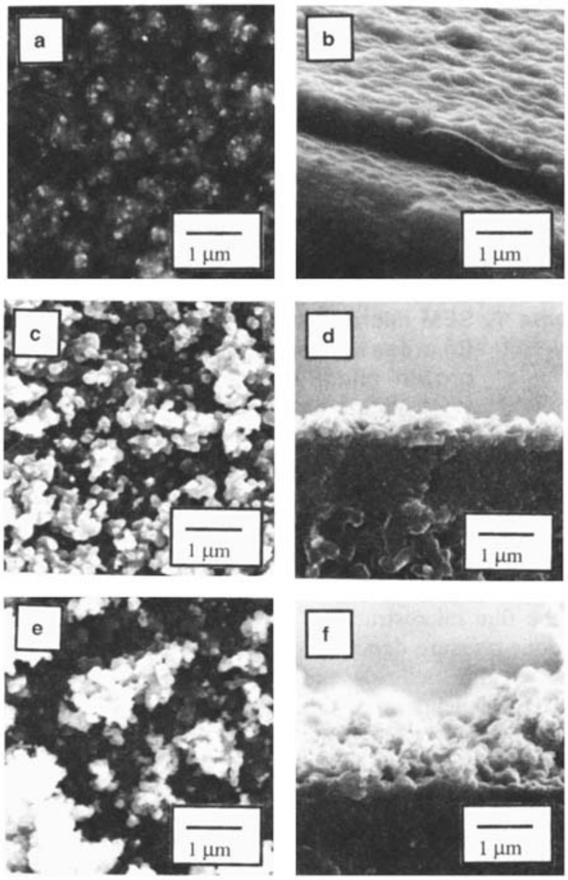

Figure 8. SEM micrographs of the film surface and cross section for a silver film deposited with (a) and (b) 6.0-m sucrose, (c) and (d) 0.246-M formaldehyde, and (e) and (f) distilled water on the shell side.

to form a dense palladium film. In this case, the grain size is about 60 nm, smaller than the crystallites shown in Figure 9a.

Palladium–silver films. Palladium and silver were codeposited from a plating solution containing 90 atomic percent palladium and 10 atomic percent silver (Table 1). Similar to the palladium plating experiment, two palladium–silver composite membranes were deposited from the *same* plating solution, one exposed to air and the other immersed in 6.0-m sucrose solution. Figures 10a and 10c compare the surface structures of the two membranes after 6 h of desposition. In air, the grains are large and close to 10 μm in diameter (Figure 10a), as compared to the micron-size grains observed in the film deposited under 6.0-m sucrose (Figure 10c). In addition, the deposits in air have a broader size distribution. The film thicknesses measured from Figures 10b and 10d are 23 and 8 μm, respectively. The corresponding XRD patterns for the two films are shown in Figure 11a, which indicate (Cullity, 1978) that palladium and silver are deposited in separate phases, and that the silver contents are 15.8 and 14.4 atomic percent, respectively.

Subjecting the films to heat treatment in hydrogen at 400°C and 2 h resulted in the formation of an alloy phase, as shown

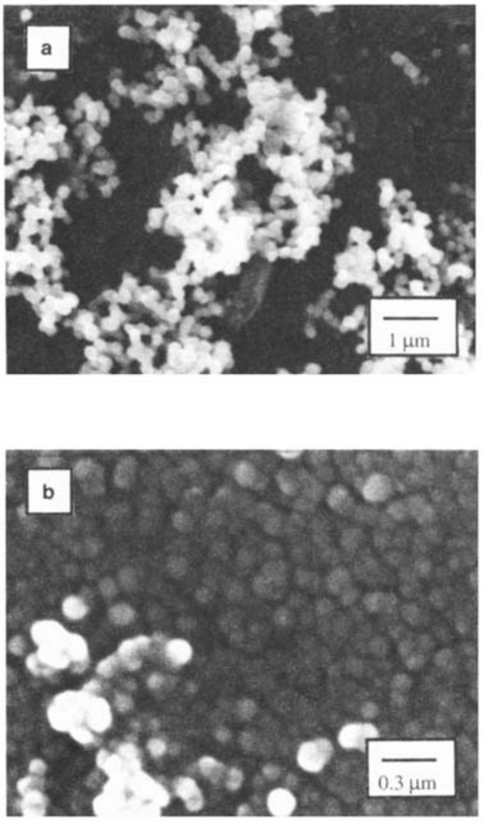

Figure 9. SEM micrographs of a palladium film deposited (a) in air, and (b) immersed in 6.0-m sucrose solution.

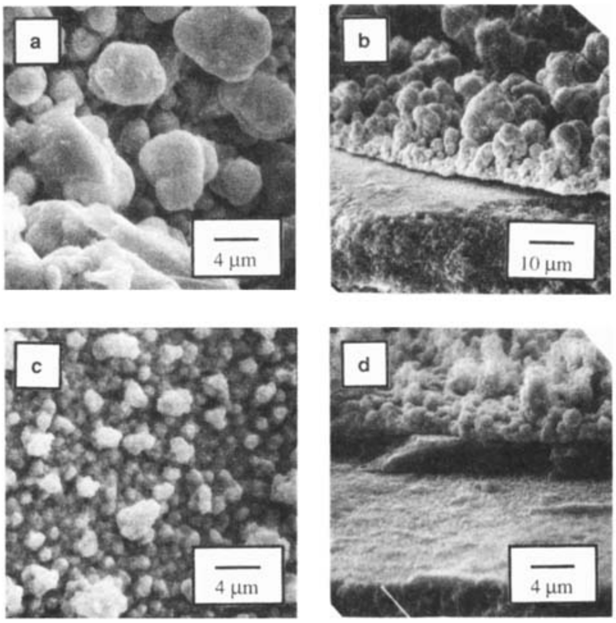

Figure 10. Surface and cross-sectional SEM micrographs of the codeposited palladium and silver films (a) and (b) in air, and (c) and (d) under 6.0-m sucrose solution.

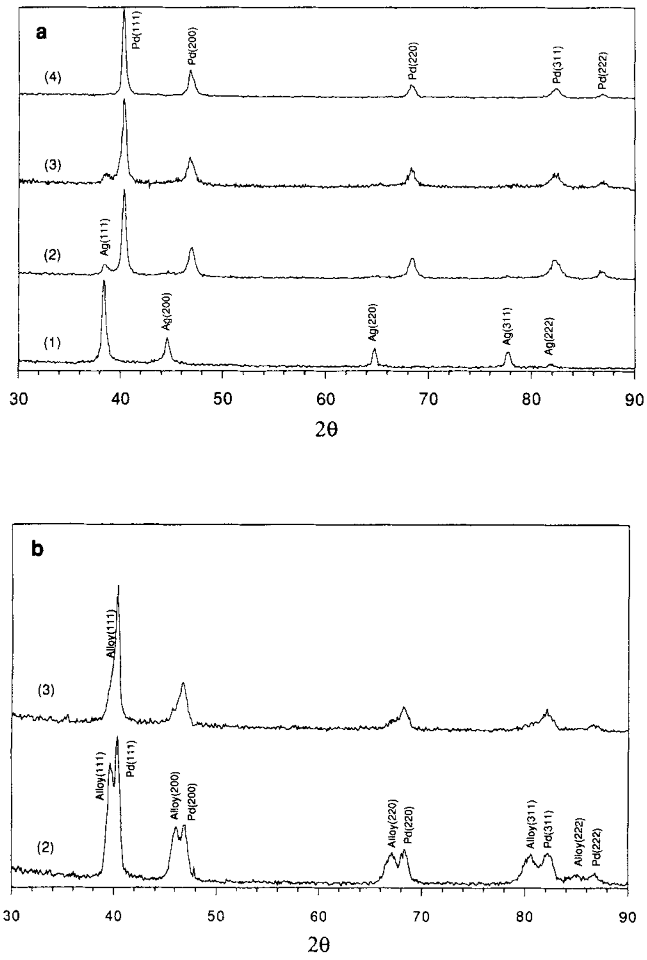

Figure 11. X-ray diffraction patterns for palladium and silver films (a) before and (b) after hydrogen heat treatment at 400°C and 2 h.

(1) Silver; (2) palladium-silver (in air); (3) palladium-silver (under 6.0-m sucrose); (4) palladium.

by the diffraction patterns in Figure 11b. It can be seen that palladium and palladium-silver alloy phases coexist in the deposit (2) after the heat treatment. The alloy phase has a lattice constant of 3.94 Å, as compared to 3.88 Å for palladium and 4.09 Å for silver. Based on the results of Yamamura et al. (1989), this lattice constant corresponds to the composition of $Pd_{69}Ag_{31}$. The peak broadening observed in the film deposited under 6.0-m sucrose (3) falls within the region for $Pd_{85}Ag_{15}$, which has a lattice constant of 3.90 Å.

The film microstructures subsequent to heat treatment in hydrogen are shown in Figure 12. The film deposited in air appears to be porous (Figure 12a) with a nonuniform size deposit. The film deposited under 6.0-m sucrose remains dense (Figure 12c) with small grains, similar to its microstructure prior to heat treatment (Figure 10c). From the cross-sectional views, it can be seen that the film deposited in air (Figure 12b) is thicker but also more porous than that deposited under 6.0-m sucrose (Figure 12d). Through porosity is evident in Figure 12a and the cross section shows a plateaulike growth. Figure 12d displays slender fingerlike growths on an otherwise dense film.

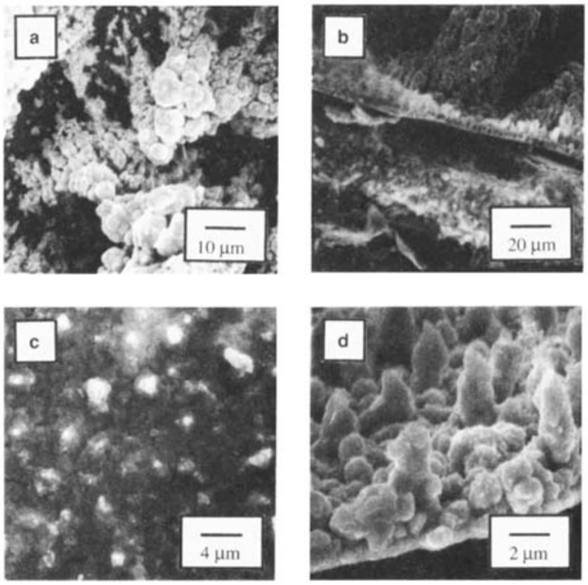

Figure 12. Surface and cross-sectional SEM micrographs of the codeposited palladium and silver film after hydrogen treatment (a) and (b) in air, and (c) and (d) under 6.0-m sucrose solution.

Thermal stability of silver films

To test the thermal stability of the silver films prepared by different techniques, the films were subjected to heat treatment under oxygen at 350°C for 55 h, and the resulting microstructures were imaged using SEM. Figure 13a shows that

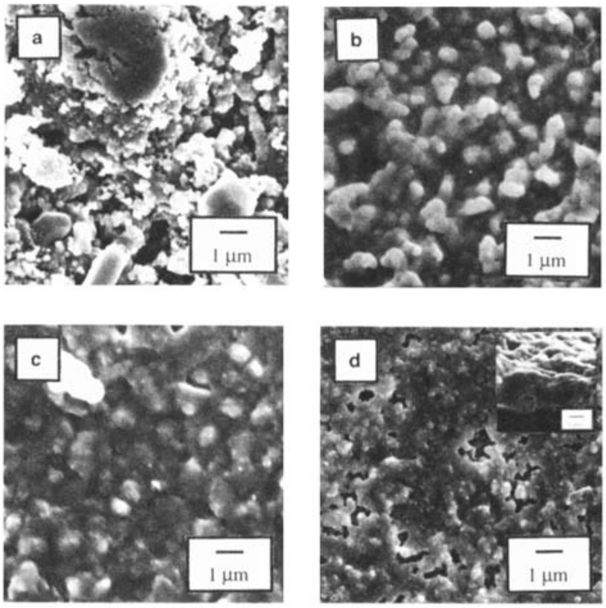

Figure 13. SEM micrographs of the silver films after heat treatment in air at 350°C and 55 h.

(a) Film of Figure 4a; (b) film of Figure 4c; (c) film of Figure 7a; (d) film of Figure 8a.

the silver film deposited in air (Figure 4a) following the heat treatment has a porous structure. It is evident that grain sintering occurred, resulting in the formation of large particles and disruption of the film integrity. Both the densified films (Figures 4c and 7a) remained dense with no observed sintering, as shown in Figures 13b and 13c, respectively. The heat treatment of film deposited by the technique of plating in the presence of osmosis (Figure 8a) showed a change in the film microstructure. As shown in Figure 13d, this film appears porous; however, an examination of the cross section (see inset) does not indicate any through porosity.

Discussion

It is clear from the results presented earlier that osmotic pressure can be used to manipulate the microstructure, porosity, and thickness of metal films supported on ceramic substrates. Three different procedures were described in the previous sections. First, an existing silver membrane (Figure 4a) was densified using the osmotic pressure created by the concentration gradient between a 6.0-m sucrose solution in the shell-side and distilled water flowing in the tube (Figure 4c). This concentration gradient results in a net flux of water from the tube-side to the shell-side, compressing the film against the γ-Al_2O_3 support. As the film is compressed, pore structure collapses increasing the film density at the expense of the film thickness (cf. Figures 4b and 4d). The film becomes denser as the pores are blocked, hence the flux of water decreases. To illustrate this further, the original and compacted films were subjected to radial osmotic pressure, but this time the pressure was directed inward. The original film peeled off from the support (Figure 5a), showing the enormous force that can be exerted by osmosis. Although the compacted film remained intact following the same experiment, it exhibited a change in microstructure (Figure 5c). Prolonging the time of film densification results in better structural stability against reverse osmotic pressure. In addition, films densified for a longer period of time have denser structure and are more stable under heat treatment (Figure 6).

By flowing a dilute plating solution inside the tube instead of water, the silver film can be densified without any decrease in its thickness. In this case, the outward flux carries the silver precursor from the solution to the tube wall, allowing it to deposit on the film while simultaneously being compressed by the osmotic pressure. This combined effect results in a denser and thicker silver film (Figure 7). However, the concentration gradient between the shell-side and tube-side is smaller because of the plating solution, resulting in a lower osmotic pressure.

The preceding techniques show how the film microstructure can be manipulated by applying osmotic pressure across an existing film. In the third method, we take advantage of the existing ceramic membrane to combine both deposition and densification steps. Since the osmotic pressure can be varied independently from the plating solution, its effect can be studied without affecting the deposition mechanism. The results show that by simply changing the shell-side concentration of solutes relative to the tube-side concentration of the plating solution, different film microstructures and thicknesses can be obtained (Figure 8). Dense or porous silver films are obtained by simply changing the direction of the osmotic pressure (cf. Figure 8a and 8e). In addition, it was shown that in the absence of osmotic pressure only a small amount of silver is deposited and the resulting film is thin and porous (Figure 8c). One may wish to compare this film to that deposited in air (cf. Figures 8c and 4a, respectively), since the osmotic pressure is also absent in the latter case. However, this comparison is not strictly correct, because capillary forces are present during deposition in air, providing the driving force for silver to deposit onto the ceramic membrane. This explains why the film deposited in air is thicker and denser than that deposited under zero osmotic pressure. For a 40-Å pore diameter, the calculated capillary pressure from Kelvin equation (Glasstone, 1940) is about 690 bar ($\gamma = 69.56$ dyne/cm, $T = 313$ K). Although this pressure is more than twice that corresponding to a 6.0-m sucrose solution, it only applies until the pore volume is filled (300 μs; Washburn, 1921). In addition, unlike the osmotic pressure, the capillary pressure depends strongly on the surface properties of the support (that is, pore size and wettability) and is therefore difficult to control.

The procedure can be used to deposit a variety of metals. For example, palladium deposited under the influence of osmotic pressure showed marked improvement over that deposited by conventional electroless plating (Figure 9). Also, palladium and silver were codeposited from an EDTA-stabilized ammine solution using hydrazine as reducing agent. As in the case of palladium, the film deposited in air had larger grains and was porous, while that deposited under osmotic pressure had smaller grains and was denser (Figure 10). Initially, separate palladium and silver phases were formed, and subsequent to heat treatment in hydrogen at 400°C for 2 h, alloy phases were detected in both cases. For the deposit in air, a $Pd_{69}Ag_{31}$ phase *coexisted* with pure palladium, whereas a *single* $Pd_{85}Ag_{15}$ phase was detected for the deposit under 6.0-m sucrose. This difference can be explained by the nature of the deposition process. Electroless plating is autocatalytic and the reaction is limited by mass transfer, hence increasing mass transfer improves deposition. During electroless plating and osmosis, the concentration gradient between the plating solution and 6.0-m sucrose results in a net outward flux toward the wall, enhancing mass transfer of precursors to the target surfaces. This has the dual effect of decreasing grain size of the film and providing intimate mixing of the two precursors that facilitates the alloying process during the heat treatment. The film deposited by conventional electroless plating yields larger grain sizes and *incomplete* alloy formation.

Silver films deposited under osmotic pressure are thermally more stable in oxygen at 350°C, as compared to films deposited in air that show local sintering leading to larger interaggregate pores and damage in microstructure. All films deposited under osmotic pressure remained dense after heat treatment, although the films deposited by simultaneous plating and osmosis showed structural changes. This could be due to the lower osmotic pressure available for compressing the film in the latter case.

Concluding Remarks

We have presented new techniques for preparing metal–ceramic composite membranes. These procedures combine electroless plating and osmosis to deposit metal films of controlled structure. There are two independent strategies that can be exploited; the first involves an optimization of the plating processes (such as solution composition, and plating time), while the second employs the proper use of osmotic pressure in order to enhance properties of the film. The techniques presented in this article are attractive not only for their wide range of application, but also because of their simplicity and potentially low capital cost.

In forthcoming articles, we will discuss in greater detail the effects of osmotic pressure and various plating parameters on the deposited film microstructure, porosity, and thickness for silver and palladium composite membranes, as well as their performance in gas separation and catalysis. Currently, we are also using the same techniques to fabricate other palladium alloy membranes.

Acknowledgments

We gratefully acknowledge financial support from the National Science Foundation (Grant CTS-9213683) and Union Carbide Chemicals and Plastics Company, Inc. We also thank Messrs. Joseph R. Royer and John M. Sebastian for conducting some of the experiments.

Literature Cited

Atkins, P. W., *Physical Chemistry*, 4th ed., Freeman, New York (1990).

Barrer, R. M., *Diffusion In and Through Solids*, Cambridge Univ. Press, Cambridge (1941).

Bhave, R. R., *Inorganic Membranes: Synthesis, Characteristics, and Applications*, Van Nostrand Reinhold, New York (1991).

Collins, J. P., and J. D. Way, "Preparation and Characterization of a Composite Palladium-Ceramic Membrane," *Ind. Eng. Chem. Res.*, **32**, 3006 (1993).

Cullity, B. D., *Elements of X-Ray Diffraction*, 2nd ed., Addison-Wesley, Reading, MA (1978).

Garner, W. E., "Osmotic Pressure," *International Critical Tables*, National Research Council, ed., McGraw-Hill, New York (1930).

Glasstone, S., *Text-Book of Physical Chemistry*, Van Nostrand, New York (1940).

Govind, R., and D. Atnoor, "Development of a Composite Palladium Membrane for Selective Hydrogen Separation at High Temperature," *Ind. Eng. Chem. Res.*, **30**, 591 (1991).

Gryaznov, V. M., O. S. Serebryannikova, M. Yu. Serov, M. M. Ermilova, A. N. Karavanov, A. P. Mischenko, and N. V. Orekhova, "Preparation and Catalysis over Palladium Composite Membranes," *Appl. Catal. A: General*, **96**, 15 (1993).

Holleck, G. L., "Diffusion and Solubility of Hydrogen in Palladium and Palladium-Silver Alloys," *J. Phys. Chem.*, **74**, 503 (1970).

Konno, M., M. Shindo, S. Sugawara, and S. Saito, "A Composite Palladium and Porous Aluminum Oxide Membrane for Hydrogen Gas Separation," *J. Memb. Sci.*, **37**, 193 (1988).

Pearlstein, F., "Electroless Plating," in *Modern Electroplating*, 3rd ed., F. A. Lowenheim, ed., Wiley-Interscience, New York (1974).

Robinson, R. A., and R. H. Stokes, *Electrolyte Solutions*, 2nd ed., Butterworths, London (1959).

Shu, J., B. P. A. Grandjean, E. Ghali, and S. Kaliaguine, "Simultaneous Deposition of Pd and Ag on Porous Stainless Steel by Electroless Plating," *J. Membr. Sci.*, **77**, 181 (1993).

Smithells, C. J., *Gases and Metals*, Chapman & Hall, London (1937).

Uemiya, S., Y. Kude, K. Sugino, N. Sato, T. Matsuda, and E. Kikuchi, "A Palladium/Porous-Glass Composite Membrane for Hydrogen Separation," *Chem. Lett.*, 1687 (1988).

Washburn, F. W., "Dynamics of Capillary Flow," *Phys. Rev.*, **17**, 273 (1921).

Weast, R. C., *CRC Handbook of Chemistry and Physics*, 67th ed., CRC Press, Boca Raton, FL (1986).

Wu, D., R. A. Outlaw, and R. L. Ash, "Glow-Discharge Enhanced Permeation of Oxygen Through Silver," *J. Appl. Phys.*, **74**, 4990 (1993).

Yamamura, M., K. Kaneda, and T. Imanaka, "Preparation of Pd-Ag Thin Films by the RF-Sputtering Method and its Catalysis for Oxidative Dehydrogenation of Allylic Alcohols," *Catal. Lett.*, **3**, 203 (1989).

Manuscript received May 19, 1994, and revision received Nov. 14, 1994.